Efficient In situ Assessment of Radiated Emissions using Time-Domain Measurements

Jordi Solé-Lloveras
EMC Barcelona
EMC Electromagnetic BCN, S.L.
Barcelona, Spain
0000-0003-1631-1172

Marco A. Azpúrua
EMC Barcelona
EMC Electromagnetic BCN, S.L.
Barcelona, Spain
0000-0001-8078-5116

Marc Aragón Homar
EMC Barcelona
EMC Electromagnetic BCN, S.L.
Barcelona, Spain
marc.aragon@emc-barcelona.com

Yasutoshi Yoshioka
Fuji Electric Europe GmbH
European Research & Technical Center
Offenbach am Main, Germany
Yasutoshi.Yoshioka@fujielectric-europe.com

Ferran Silva
Grup de Compatibilitat Electromagnètica
Universitat Politècnica de Catalunya
Barcelona, Spain
0000-0003-3019-3993

***Abstract*—This paper presents three different case studies where the electromagnetic emissions of atypical equipment (a photovoltaic system, a passenger boarding bridge and a pallet washing machine) have been assessed in situ using time-domain measurement systems. The magnetic field (150 kHz-30 MHz) and electric field (30 MHz-1 GHz) emissions are considered. The technical challenges encountered and the solutions adopted for each scenario will be highlighted by describing the methodology employed. The goal is to relate the empirical knowledge and know-how gained through those study cases with the specific requirements and procedures defined in the standards. In that sense, multi-channel time-domain emissions measurements have been essential to carry out those measurement campaigns efficiently. The results are summarised as lessons learned during the experiences reported in this article. This work is relevant to support the revision or development of standards about in situ EMC testing as it provides helpful evidence to validate alternative radiated emissions measurement methods under realistic conditions.**

***Index Terms*—electromagnetic compatibility, electromagnetic emissions, in situ, time-domain measurements, standards.**

I. Introduction

All electronic equipment within the European market must comply with the essential requirements of the European EMC directive [1]. It covers all types of products, including what has been called atypical equipment, that is, a subset of devices and systems that can't be tested in standard EMC laboratory conditions because of (large) size, (high) power, safety and (complex) installation constraints. Examples of atypical equipment are photovoltaic systems [2], wind turbines [3], automatic storage systems [4], and rolling stocks [5].

When it is impossible to measure the emissions of atypical equipment in a standard test site, the in situ approach is the only viable alternative. Nevertheless, numerous drawbacks of performing in situ measurements should be considered. The main one is the uncontrollable conditions of the test site, as measurements may be performed within a non-clean and reflective electromagnetic environment. Detecting the disturbances produced by the equipment under test (EUT) can be challenging without shielding to attenuate signals and noise generated in the surroundings [3], [6]. Other challenges of in situ emissions assessments arise from the high number of measurement points/conditions that may imply lengthy and costly campaigns. Therefore, more sophisticated yet efficient and agile means of detecting emissions should be used.

However, to date, only a few standards cover in situ EMC testing of atypical equipment. The most general one is CISPR 11 [7], which is concerned with industrial, scientific, and medical equipment. Moreover, the CISPR 37 [8] is being developed by the CIS/B Working Group 7 (WG7) and focuses on in situ testing of atypical equipment. It is expected this situation will change as more product standards are gaining interest towards better and more practical procedures for in situ emissions testing, e.g. the IEC 61400-40 [9] for wind energy generation systems and the IEC 62920 [10] for PV generating systems. In this regard, to support the work of the corresponding standardisation committees, it is crucial to exercise the proposed emissions measurement methodologies under realistic situations and to identify means, tools and strategies to overcome the difficulties found in the "on-site" conditions. Hence, this article gathers knowledge from our experience using time-domain emissions measurement systems in situ through representative study cases.

The rest of the paper is organised as follows: In Section II, we describe the methodology employed during the in situ measurements, including procedural considerations and a brief overview of the multi-channel time-domain EMI measurement systems. Subsequently, Section III present the radiated emissions from a photovoltaic system, a passenger boarding bridge and a pallet washing machine as case studies. Next, Section IV summarises the lessons learned from the experiences reported and leads to our final thoughts regarding the relevance of this work for validating alternative emissions test methods under realistic conditions.

II. METHODOLOGY

A. Measurement method and practical considerations

Measurements are performed in open, unshielded environments and under the influence of electromagnetic disturbances of all types: wireless communications, broadcasting, as well as other electronic devices. To discern the contribution of the EUT, a measurement is conducted with the equipment switched off (ambient level measurement) and then compared with a measurement with the equipment in operation. Measures are taken at least at 3 points on different axes in order to find the side of the EUT with higher emissions. According to the CISPR 11 standard, for class A group 1 equipment (all of the studied cases are within this group), the measurement distance is $30\,\mathrm{m}$. Nevertheless, in the CISPR 37 draft, the reference distance is set to $10\,\mathrm{m}$ and any measurement distance larger than $3\,\mathrm{m}$ is allowed considering a correction factor. The latter criterion is beneficial for in situ because it is not always possible to measure at a certain fixed distance. Additionally, the CISPR 37 draft describes a procedure to define the EUT boundary (Fig. 1) when it encompasses different elements, for example, in the case of a photovoltaic system, where there are solar panels and an inverter. This is used to determine the standard distance between the EUT and the antenna.

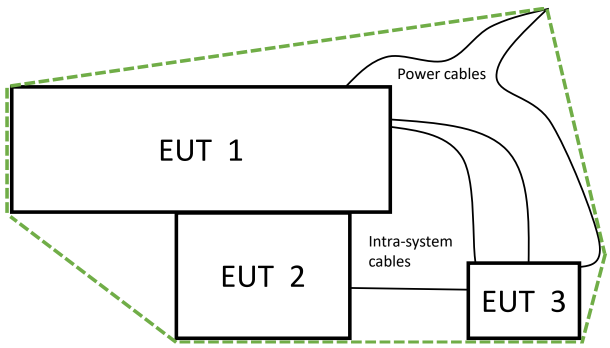

Fig. 1. Boundary determination for a multi-unit EUT according to CISPR 37. The measurement distance is referenced to the boundary outlined in green.

The usual frequency range assessed goes from $150\,\mathrm{kHz}$ to $30\,\mathrm{MHz}$ for magnetic field emissions and from $30\,\mathrm{MHz}$ to $1\,\mathrm{GHz}$ for electric field emissions. For the magnetic field, a loop antenna in three different axes (x, y, and z) at the height of $2\,\mathrm{m}$. For the electric field, a biconical antenna is employed for the range of $30\,\mathrm{MHz}$ to $200\,\mathrm{MHz}$ and a log-periodic antenna for the $200\,\mathrm{MHz}$ to $1\,\mathrm{GHz}$ range. Both polarities (vertical and horizontal) are evaluated while maintaining a height of $1\,\mathrm{m}$. In the last two cases, the antennas are connected to a $30\,\mathrm{dB}$ preamplifier to achieve a higher sensitivity.

B. Multi-channel time-domain EMI measurement systems

Alternative EMI receiver implementations have been created for measuring and analyzing electromagnetic emissions from complex systems in the time domain using multiple channels [11], [12]. Commonly, these complex systems have behaviour that changes over time, and various modes of operation during normal functioning [4], [5]. Because of this, the emission signature of the system being tested can vary during measurement, making the frequency-swept measurement method unreliable. Moreover, when assessing emissions of atypical equipment in situ, the signals and the radiofrequency noise in the environment add further uncertainty to measurements making it even more relevant to consider the time-domain information as part of the emissions assessment [6]. Therefore, time-domain EMI measurement systems are well-suited for in situ emissions assessment.

Advanced EMI receivers with multi-domain and multi-channel capabilities can be used (Fig. 2) to cope with those challenges. In this context, multi-domain means EMI measurements are processed and analysed in time, frequency, and statistical domains, independently or simultaneously. This allows for accurate spectral estimations according to standard specification [13], [14] and complementary analysis, including waveform measurements, spectrograms, waterfall/persistence plots, and probabilistic information about the interference, e.g., the amplitude probability distribution function. Moreover, multi-channel means the instrument has several inputs. Therefore, it can perform the acquisitions synchronously, given a triggering event. Those analysis capabilities beyond the standard emissions requirements have proven to be highly valuable for interference evaluation, for instance, in wireless systems [15], [16].

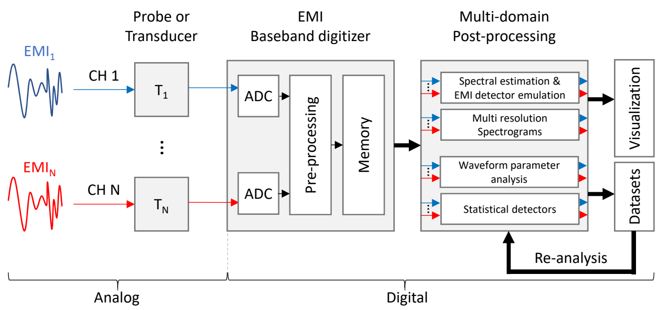

Fig. 2. Block diagram of the multi-channel time-domain EMI measurement system used during the experiments.

For the measurements covered in Section III we used a multi-channel time-domain EMI measurement system compatible with flexible resolution deep memory oscilloscopes. Welch's method is used for spectral estimation, and adaptive windowing functions are used to set any required resolution bandwidth. For H-field emissions, the hardware used was the 4-channels USB oscilloscope PicoScope 5444B from Pico Technology. It has up to $16\,\mathrm{bit}$ vertical resolution, $1\,\mathrm{GSa/s}$ of maximum sampling rate, $200\,\mathrm{MHz}$ bandwidth, and memory of $512\,\mathrm{MSa}$. With this configuration, CISPR 16-1-1 baseline requirements are met for CISPR bands A and B [12], [13]. Conversely, a 4-channel Digital Real-time Oscilloscope Tektronix 5104B was employed for E-field measurements. It has a maximum sampling rate of $10\,\mathrm{GSa/s}$ and a bandwidth of $1\,\mathrm{GHz}$ with frequency response correction.

III. Case studies

In this section, we summarise the main results, challenges encountered and experiences with in situ measurements in three well-defined scenarios: a complete photovoltaic (PV) system, an airport passenger boarding bridge and finally, an industrial pallet washing machine.

A. Case study 1: Photovoltaic system

The first case of study is a PV system. This system's constituent elements are a $2\,\mathrm{kW}$ scaled-down prototype of an inverter which models a $500\,\mathrm{kW}$ grid-connected PV inverter, 12 solar panels and AC power sources simulating the AC grid. A provisional outdoor facility is deployed to evaluate the system under natural illumination conditions (Fig. 3).

Fig. 3. Case study 1. System under test in the outdoor test site. The photo shows the DC-AC inverter with 12 PV panels behind it.

This experiment was designed to try alternative measurement methodologies, not as an actual test for certifying compliance. The measurements were deployed in a parking lot in Magdeburg, Germany. The wiring and the installation are not meant to be representative of an actual professional one. Sources of electromagnetic disturbances in the surroundings influenced the measurements, in particular, an electric vehicle charger located at $30\,\mathrm{m}$ from the EUT and a tram stop located approximately at a distance of $70\,\mathrm{m}$.

Here the primary interest is to evaluate the magnetic field emissions, which are measured from $9\,\mathrm{kHz}$ up to $30\,\mathrm{MHz}$. The Picoscope 5444B was used as the measuring device. RF cables, connectors and transitions were transported with the oscilloscope in a hand-carried suitcase. Antennas were provided by the host where the experiments were conducted.

Due to the site constraints, only a few points were defined to evaluate the emissions at different orientations. This subsection presents a couple of relevant cases, showing the functionality of the time domain compact measurement system. In the first example, the magnetic field is measured at a distance of $30\,\mathrm{m}$ from the equipment (setup in Fig. 4).

Keeping the loop antenna (Schwarzbeck FMZB 1513) in the same position, two measurements are conducted, one with the device powered off and one with the device in operation. The H-field's x-, y-, and z- orientations of the magnetic field are considered at every measurement point. The ambient level measurement with the equipment switched off is used to determine the environmental electromagnetic interference of the test site. Results are compared in Fig. 5.

Fig. 4. Setup used for in situ magnetic field measurements for the PV system (Case study 1). Distance to the EUT is $30\,\mathrm{m}$. Buildings may have an influence on the measurements, however this was out of the scope of this study.

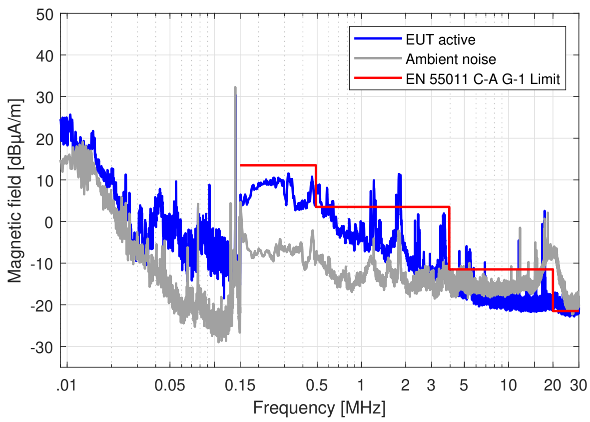

Fig. 5. Magnetic field strength measured along the z-axis (H_z) at $30\,\mathrm{m}$ distance from the EUT (Case study 1).

A rise in received magnetic field intensity is detected when the EUT is turned on. The test had to be repeated several times, as narrow band components appeared around $80\,\mathrm{kHz}$ in some measurements. It turned out this contribution was from the braking and start-up of the tramway in the station close to the test site. However, as measurements were performed in real-time, this situation was identified and solved by repeating fully compliant acquisitions every second. Additionally, measurements at a $10\,\mathrm{m}$ distance were taken to obtain a more precise comparison of the contribution of the EUT in relation to the ambient noise levels (Fig. 6). This time, a narrow component is seen at $f_0 = 92\,\mathrm{kHz}$ along with its harmonics above $300\,\mathrm{kHz}$. In the previous case, at $30\,\mathrm{m}$ (Fig. 5), the peak at f_0 also appeared but with a smaller magnitude. Note also the higher amplitude of the narrowband disturbance at $138\,\mathrm{kHz}$, which is increased by $20\,\mathrm{dB}$. Nevertheless, as this peak appears in the ambient measurements, it does not correspond to the EUT. In other words, we are approaching the unrecognised noise source instead. It is meaningful to perform investigative measurements at closer distances than the standard one in order to identify whether the different spectral components are produced by the EUT, or by unrecognised elements in the surroundings.

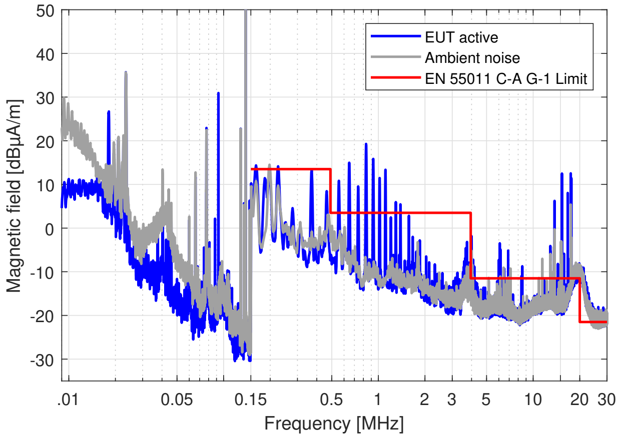

Fig. 6. Magnetic field strength measured along the x-axis at $10\,\mathrm{m}$ distance (Case study 1).

B. *Case study 2: Passenger boarding bridge*

The second scenario is a passenger boarding bridge intended for airport use. The test site is the actual facility where it is manufactured before being transported to the end customer. The maximum length of the EUT is $38\,\mathrm{m}$ and it has several electrical panels, touch screens, controls and motors. The reference point for measuring the distance from the antenna to the EUT is the midpoint between the cockpit and the main movement engine. An image of the EUT with a loop antenna at a distance of $30\,\mathrm{m}$ is shown in Fig. 7.

Fig. 7. Case study 2. Photo of the in situ setup for magnetic field emissions measurements from a passenger boarding bridge.

The contribution of the EUT with respect to the ambient noise is noticeable even at $30\,\mathrm{m}$, as shown in the $150\,\mathrm{kHz}$ - $300\,\mathrm{kHz}$ range (Fig. 8). Initially, it was assumed this broadband emission was due to the motion system when the passenger boarding bridge performs short translations forward and backwards. Nonetheless, after several repetitions, we observed that such disturbances were not produced in some cases. It was found that while our measurements were run, a group of technicians were working on another passenger boarding bridge. In other words, time-domain measures helped identify fluctuations in ambient noise levels that otherwise may have led to false assumptions. This is why it is essential to perform several measures to characterise the electromagnetic environment better and provide more confidence regarding the assessment's conclusions. That is, to ensure the disturbances reported are produced by the EUT and not by uncontrolled nearby elements in the surroundings.

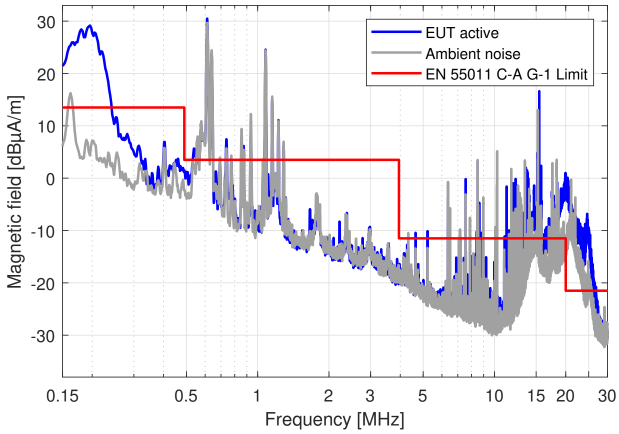

Fig. 8. Magnetic field strength measured along the x-axis at $30\,\mathrm{m}$ distance (Case study 2).

The electric field is measured at a $10\,\mathrm{m}$ distance in order to achieve a higher signal-to-noise ratio after no significant detection was possible at $30\,\mathrm{m}$. In this case, and after repeating several measures in the same working mode, broadband emissions from $40\,\mathrm{MHz}$ up to $300\,\mathrm{MHz}$ are detected, as depicted in Fig. 9.

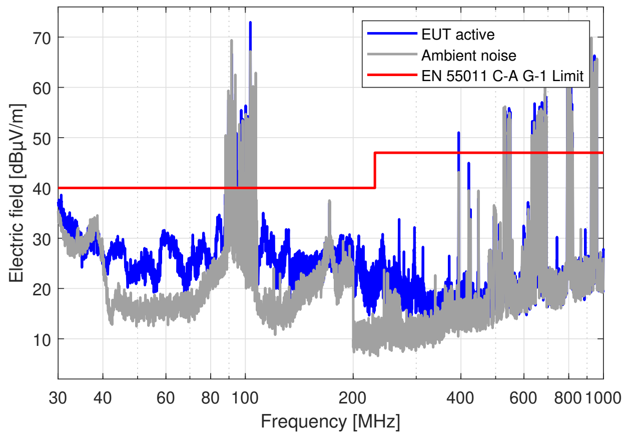

Fig. 9. Electric field emissions measured at 10m distance in horizontal polarization (Case study 2).

C. Case study 3: Pallet washing tunnel

The last study case is a pallet washing tunnel machine (Fig. 10). It consists of a conveyor belt through which the pallets enter to be cleaned and rinsed. The main electrical/electronic elements that can cause electromagnetic disturbances are the motors (wash and bilge pumps and the drag chain), motor drivers, electric heaters, electro-valves, and an interface display.

Fig. 10. Case study 3. A pallet washing tunnel.

The most interesting aspect of this in situ test is the test site itself, an industrial warehouse approximately 54 m long and 30 m wide, with no other machinery or electronic equipment active during the test. The test site ensures an obstacle-free distance of more than 30 m.

An image of the test site with the antenna placed at 30 m is shown in Fig. 11. To evaluate the different faces of the equipment, the EUT was rotated every 90º with the help of a forklift. At the same time, this was helpful because the measurement axis remained the same.

Fig. 11. Setup used for in situ radiated field emissions measurements from the pallet washing tunnel in an industrial warehouse (Case study 3).

Several measurements are performed at 30 m, 10 m and 3 m. Regarding results obtained at 30 m, it was not possible to identify the EUT emissions from the ambient levels, so a shorter distance was used. Then, the antenna is placed at a distance of 10 m, and the front face of the EUT is oriented to the front of the antenna. No noticeable variation in the measured spectrum is observed. Nevertheless, when rotating the EUT 90º counterclockwise, the side where the main electronics of the EUT are located, some low-level broadband emission between 200 MHz and 300 MHz is detected (Fig. 12).

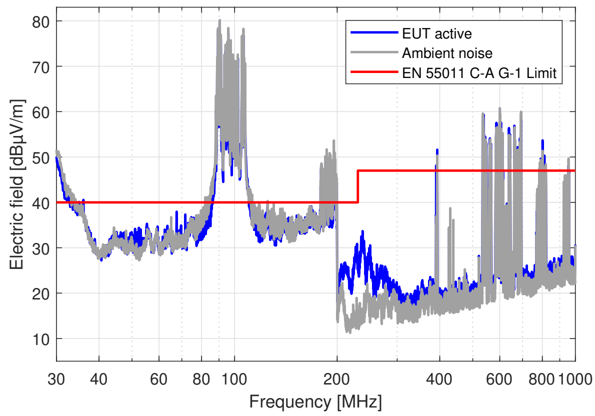

Fig. 12. E-field emissions measured at 10 m distance in horizontal polarization and with the pallet washing tunnel rotated 90º counterclockwise (Case study 3).

Subsequently, the antenna is placed at 3 m from the equipment, maintaining the same measurement axis. It must be noticed that at 3 m, the measurements are not in far-field conditions. Therefore, such measurements were only intended to corroborate the source of the emissions was the EUT. Results are illustrated in Fig. 13. As expected, there is an increase of magnitude in the broadband emissions registered in the 200 MHz - 300 MHz band and, additionally, the field strength level between 50 MHz and 60 MHz also rises.

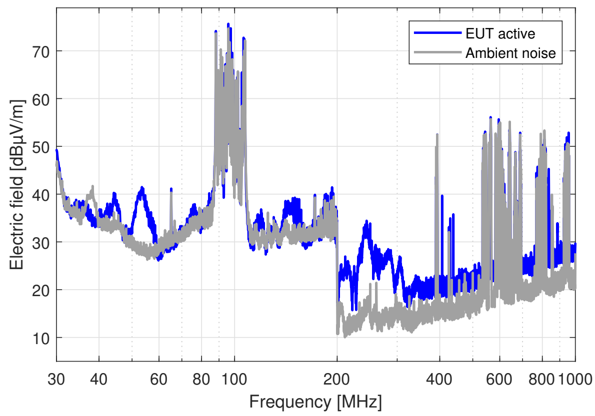

Fig. 13. E-field emissions at 3 m distance in horizontal polarization (Case study 3).

IV. Lessons Learned

Several lessons are drawn based on the experience gained and the different scenarios studied to improve the in situ radiated emissions methodology. Some of them, if not the most relevant to bear in mind, are the following:

- The ambient levels are changing over time. It is highly likely that the two consecutive emission measurements differ substantially due to the time-varying ambient noise. This especially occurs when other equipments in the surroundings are prone to generate disturbances. It is important to identify the different noise sources in the spectrum and to minimise the operation of nearby electronic/electrical devices. For this purpose, FFT-based receivers with real-time capabilities are convenient.
- Due to the relatively high field intensity of broadcasting and communication services in the environment, specific bands will inherently be well above the limits. In such conditions, according to CISPR 11, it is necessary to compare if the field strength in the frequency bands surpassing the limits is increased when the EUT is operating to determine if the EUT complies with the emissions requirement. Beyond that, time domain measurements can be helpful for decomposing broadband from narrowband signals in the time domain thus providing some degree of ambient noise cancellation. Multichannel time-domain measurement systems facilitate the correlation between conducted, near-field and far-field phenomena, which is key in the investigation process.
- The fast time-domain measurements are advantageous for equipment whose operation mode does not allow a continuous cycle. In the passenger boarding bridge, which made $20\,\mathrm{s}$ motion sequences with a progressive movement, we acquired data corresponding to a given position and state. If the measurement had been made with a spectrum analyser, each frequency would have been associated with the variable EUT positions and power consumption, thus delivering misleading results.
- Most of the time, at $30\,\mathrm{m}$, the EUT emissions can hardly be discerned from the ambient noise, in particular for E-field measurements. At such a distance, it is probable that some disturbances detected are caused by external elements which are closer to the antenna than the EUT itself. Hence, it is necessary to reduce the measurement distance, at least, to check that the magnitude of the detected disturbances increases in relation to the $30\,\mathrm{m}$ distance and that they are indeed produced by the EUT.

ACKNOWLEDGMENT

The project (21NRM06 EMC-STD) has received funding from the European Partnership on Metrology, co-financed by the European Union's Horizon Europe Research and Innovation Programme and by the Participating States.

EMC Barcelona's project under grant number SNEO-20211223 has received funding from CDTI, which is supported by "Ministerio de Ciencia e Innovación" and financed by the European Union – NextGenerationEU – through the guidelines included in the "Plan de Recuperación, Transformación y Resiliencia".

Dr. Azpúrua has received funding from the StandICT.eu 2023 project, financed by the European Union's Horizon Europe - Research and Innovation Programme - under grant agreement no. 951972.

REFERENCES

[1] *Directive 2014/30/EU of the European Parliament and of the Council of 26 February 2014 on the harmonisation of the laws of the Member States relating to electromagnetic compatibility.*

[2] S. Linder and K. Wiklundh, "In-situ Measurements of Conducted and Radiated Emissions from Photovoltaic Installations," in *2022 International Symposium on Electromagnetic Compatibility – EMC Europe*, 2022. doi: 10.1109/EMCEurope51680.2022.9901001 pp. 231–236.

[3] T. Groß and J. Medler, "Advanced analysis for separation of ambient and device under test emission for in-situ measurements," in *2020 IEEE International Symposium on Electromagnetic Compatibility & Signal/Power Integrity (EMCSI)*, 2020. doi: 10.1109/EMCSI38923.2020.9191454 pp. 553–556.

[4] M. Pous, M. Azpúrua, and F. Silva, "Benefits of Full Time-Domain EMI Measurements for Large Fixed Installation," in *2016 International Symposium on Electromagnetic Compatibility - EMC EUROPE*, 2016. doi: 10.1109/EMCEurope.2016.7739221 pp. 514–519.

[5] M. Pous, M. A. Azpúrua, J. A. Oliva, M. Aragón, I. González, and F. Silva, "Full time domain emi measurement system applied to railway emissions according to iec 62236-3-1/en 50121-3-1 standards," in *2018 International Symposium on Electromagnetic Compatibility (EMC EUROPE)*, 2018. doi: 10.1109/EMCEurope.2018.8485173 pp. 260–265.

[6] M. A. Azpúrua, M. Pous, and F. Silva, "A Single Antenna Ambient Noise Cancellation Method for In-situ Radiated EMI Measurements in the Time-Domain," in *2016 International Symposium on Electromagnetic Compatibility - EMC EUROPE*, 2016. doi: 10.1109/EMCEurope.2016.7739185 pp. 501–506.

[7] "CISPR 11 Ed. 5: Industrial, scientific and medical equipment - Radio-frequency disturbance characteristics - Limits and methods of measurement," Comité International Spécial des Perturbations Radioélectriques, Geneva, CH, Standard, 2009.

[8] "Committee draft - CISPR 37 ED 1: Industrial, scientific and medical equipment - Radio-frequency disturbances characteristics - Limits and methods for measurements in situ and at defined sites." Comité International Spécial des Perturbations Radioélectriques, Geneva, CH, Standard, Dec. 2021.

[9] "IEC 61400-40 ED1: Wind energy generation systems - Part 40: Electromagnetic Compatibility (EMC) - Requirements and test method." IEC, Geneva, CH, Standard, 2018.

[10] "IEC 62920:2017. Photovoltaic power generating systems - EMC requirements and test methods for power conversion equipment." IEC, Geneva, CH, Standard, 2017.

[11] M. A. Azpúrua, M. Pous, and F. Silva, "A Measurement System for Radiated Transient Electromagnetic Interference based on General Purpose Instruments," in *2015 IEEE International Symposium on Electromagnetic Compatibility (EMC)*, 2015. doi: 10.1109/ISEMC.2015.7256338 pp. 1189–1194.

[12] M. A. Azpúrua, M. Pous, J. A. Oliva, B. Pinter, M. Hudlička, and F. Silva, "Waveform Approach for Assessing Conformity of CISPR 16-1-1 Measuring Receivers," *IEEE Transactions on Instrumentation and Measurement*, vol. 67, no. 5, pp. 1187–1198, 2018. doi: 10.1109/TIM.2018.2794941

[13] M. A. Azpúrua, M. Pous, and F. Silva, "Specifying the Waveforms for the Calibration of CISPR 16-1-1 Measuring Receivers," *IEEE Transactions on Electromagnetic Compatibility*, vol. 62, no. 3, pp. 654–662, 2020. doi: 10.1109/TEMC.2019.2923813

[14] M. A. Azpúrua, M. Pous, M. Fernandez, and F. Silva, "Dynamic Performance Evaluation of Full Time Domain EMI Measurement Systems," in *2018 International Symposium on Electromagnetic Compatibility (EMC EUROPE)*, 2018. doi: 10.1109/EMCEurope.2018.8485086 pp. 561–566.

[15] M. Pous, M. A. Azpúrua, and F. Silva, "Measurement and Evaluation Techniques to Estimate the Degradation Produced by the Radiated Transients Interference to the GSM System," *IEEE Transactions on Electromagnetic Compatibility*, vol. 57, no. 6, pp. 1382–1390, 2015. doi: 10.1109/TEMC.2015.2472983

[16] K. Wiklundh, "Relation between the Amplitude Probability Distribution of an Interfering Signal and its impact on Digital Radio Receivers," *IEEE Transactions on Electromagnetic Compatibility*, vol. 48, no. 3, pp. 537–544, 2006. doi: 10.1109/TEMC.2006.877782